Bedenikovic, T.
Osaka J. Math.
48 (2011), 99–125

ASPHERICITY RESULTS FOR RIBBON DISK COMPLEMENTS VIA ALTERNATE DESCRIPTIONS

TONY BEDENIKOVIC

(Received June 3, 2009, revised September 24, 2009)

Abstract

An alternate description for ribbon disk complements in the 4-ball is provided. It is known (and reestablished) that this description is equivalent to the standard LOT description, up to 3-deformation. Amenable to geometric arguments, the alternate description yields asphericity results for ribbon disk complements using simple graph-theoretic criteria and, later, using a relative homotopy group which arises naturally. In the course of making and modifying the description, two algorithms are given for presenting ribbon disk groups.

1. Introduction

A *ribbon* is an immersed 2-dimensional disk in S^3 whose boundary is a p.l. knot and whose self-intersections are *ribbon-like*, meaning they are of the type illustrated in Fig. 1. In particular, the singular set for a ribbon immersion $\rho\colon B^2 \to S^3$ consists of pairs of arcs in B^2, each pair comprised of a large, properly-embedded arc and a small, interior arc. Examples of ribbons are shown in Fig. 2.

A *ribbon disk* is a properly embedded p.l. disk in the 4-ball, B^4, whose projection onto $S^3 = \mathrm{Bd}(B^4)$ is a ribbon. Slides along a collar on $\mathrm{Bd}(B^4)$ account for the morphing of ribbons to ribbon disks. For a thorough discussion of ribbons and ribbon disks, see [1] and [7].

In [7] Howie describes 2-dimensional spines for ribbon disk complements via labeled oriented trees. A review of Howie's spines, called *LOT spines*, is included in Appendix B of this article. LOT spines illuminate striking similarities between ribbon disk complements in B^4 and classical knot complements in S^3. For example, presentations for ribbon disk groups based on LOT spines strongly resemble Wirtinger presentations for knot groups. Furthermore, LOT spines, like knot complement spines, are seen to be subcomplexes of contractible 2-complexes. In light of such similarities, it is not surprising that the questions which ribbon disk complements invoke are similar to esteemed questions concerning knot complements. Foremost is the question: Are they aspherical? Indeed, many ribbon disk complements share the homotopy class of a knot complement and are thus aspherical. Not all ribbon disk complements enjoy this status

1991 Mathematics Subject Classification. Primary 57M20, 57Q99; Secondary 20F99.

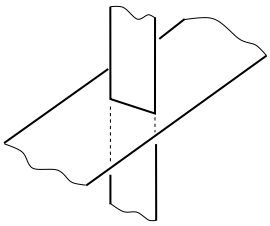

Fig. 1. A ribbon-like intersection.

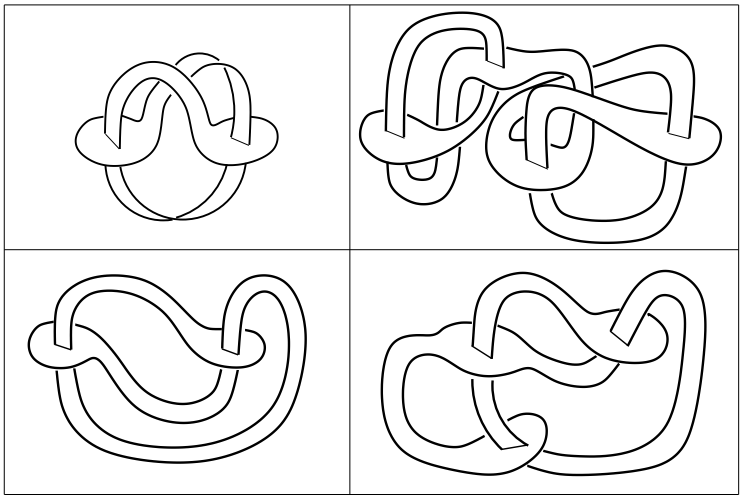

Fig. 2. Pages from a catalog of ribbons.

[7] and [11], however, and the question of asphericity remains open. In this way ribbon disk complements play an important role in the investigation of Whitehead's question whether every subcomplex of an aspherical 2-complex is itself aspherical [14] and [6].

In Section 2 of this article an alternate description to the LOT description is provided. The main result in this regard is

Theorem 2.1. *A ribbon disk complement in* B^4 *can be described as a* 3*-complex of the form*

$$[U \setminus \Gamma] \cup c * \mathrm{Bd}(U),$$

where U *is a* 3*-dimensional cube with handles and* Γ *is an interior graph in* U*. The graph* Γ *contains the original ribbon knot and is obtained by attaching spanning arcs to the ribbon knot, one spanning arc for each ribbon singularity.*

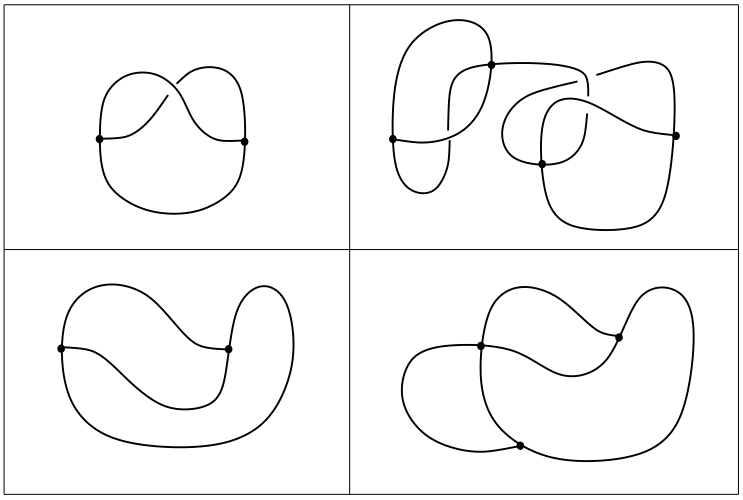

Fig. 3. Corresponding core graphs for the ribbons above.

This description for the ribbon disk complement is based on work by Robert Craggs, which tells a more general story of 2-complexes in 4-manifolds. Here, the description is presented as it applies to ribbon disk complements. For the reader's benefit, motivation for this description is provided in Appendix A. In [3, Chapter 2], Cavagnaro shows that this description is equivalent to the standard LOT description, up to 3-deformation. This equivalence is (re)established in Appendix B of this article. The proof is the author's own and follows quickly from earlier observations.

The description in Theorem 2.1 is further modified to obtain a 2-dimensional spine for the ribbon disk complement, from which a presentation for the ribbon disk group can be written. To this end, the notion of a *core graph* is helpful. Define a core graph for a ribbon to be any 1-dimensional spine for the ribbon whose vertex set contains precisely one point from each singular arc of the ribbon. One may, for example, thicken the ribbon to a cube with handles, then identify a 1-dimensional core, being sure to place vertices on the ribbon's singular arcs. In this way, the vertices of the core graph correspond to ribbon singularities and the edges of the core graph correspond to 1-handles in a thickening of the ribbon. Fig. 3 illustrates examples of core graphs.

It may be assumed, without changing the 3-deformation type of the complement, that the LOT for a ribbon is a chain, that is, a tree with precisely two extremal vertices [7, Proposition 4.1]. Consequently, it may be assumed that a core graph has precisely two vertices of valence 3 and that its remaining vertices have valence 4. In particular, the chain assumption allows the small arcs in the singular set of the ribbon immersion to be ordered left to right in B^2. The leftmost small arc, then, corresponds to one vertex of valence 3 in the core graph; the rightmost small arc to the other vertex of valence 3. All intermediate small arcs correspond to vertices of valence 4. This

arrangement for core graphs will be assumed throughout.

Further, an edge's position at a vertex of a core graph will be important. Each vertex in the core graph, therefore, will be said to have a top edge, a bottom edge, and either one or two side edges, depending on its valence. Labels will be placed on ends of edges at a vertex and these labels play the central role in writing a presentation for the ribbon disk group.

In Section 3 the language of the core graph is used to state two asphericity results for ribbon disk complements, both based on simple, graph-theoretic criteria. The first result establishes asphericity provided a certain subgraph of a twist-free core graph is a forest. (Intuitively, a twist-free core graph corresponds to a ribbon without half-twists.)

Theorem 3.1. *Suppose all edges containing a bottom label are deleted from a twist-free core graph. If the graph which remains is a forest, then the ribbon disk complement is aspherical.*

The second result establishes asphericity provided the core graph has a particular cut-edge property. This result may be viewed as a topological analog of a well-known algebraic result in the subject.

Theorem 3.2. *Suppose a core graph C can be written as $C = A \cup e \cup B$, where A, B are disjoint core graphs and e is an edge which connects them. If A and B correspond to aspherical ribbon disk complements, then C corresponds to an aspherical ribbon disk complement.*

In Section 4 the main description for the ribbon disk complement is modified by eliminating the cone from the description. In this setting the ribbon disk is complement described as the ribbon graph complement $S^3 \setminus \Gamma$ with 2-cells attached along a complete set of meridional curves in $\mathrm{Bd}(U)$. Recall that U is a regular neighborhood of the ribbon in S^3 and Γ is an interior graph comprised of the ribbon knot and spanning arcs. A modification in this direction suggests a second algorithm for presenting a ribbon disk group. The presentation in this case is a relative presentation with respect to a standard Wirtinger presentation for $\pi_1(S^3 \setminus \Gamma)$.

Furthermore, this approach suggests a natural pair of spaces to consider: the ribbon disk complement itself and the ribbon graph complement $S^3 \setminus \Gamma$ which is a subset of it. Using the homotopy sequence of the pair, an asphericity result is obtained based on the second relative homotopy group.

Theorem 4.1. *Let $Y = [S^3 \setminus \Gamma] \cup \{E_1, E_2, \ldots, E_n\}$ denote the ribbon disk complement as described above and let X be the subspace $S^3 \setminus \Gamma$. If $\pi_2(Y, X)$ is a free group, then Y is aspherical.*

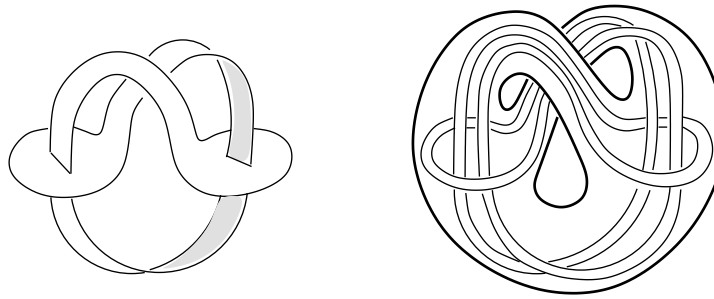

Fig. 4. An example of a ribbon and corresponding 3-manifold W.

Empirical evidence suggests this condition is necessary and sufficient for a sizable subset of ribbon disk complements.

2. An alternate description for ribbon disk complements

Fix a collar $S^3 \times I$ on the boundary of B^4 and consider a ribbon disk embedded in the collar. Recall that the ribbon disk projects along the fibers of the collar onto a ribbon in $S^3 \times \{0\}$. To begin the alternate description for the ribbon disk complement, let U denote a regular neighborhood of the ribbon in $S^3 \times \{0\}$. Notice that U is a 3-dimensional cube with handles and that the boundary of the ribbon disk, which is a ribbon knot, resides in its interior. It may be assumed without loss of generality that U is Heegaard in S^3. Let W denote the 3-manifold obtained by removing from U the interior of a small regular neighborhood of the ribbon knot, as illustrated in Fig. 4.

Next, add to W the cone over $\mathrm{Bd}(U)$ to obtain the 3-complex

$$W \cup c * \mathrm{Bd}(U).$$

The description for the ribbon disk complement is completed by adding 3-cells to this 3-complex, one 3-cell for each ribbon singularity, according to the instructions which follow.

Let $S_1, S_2, \ldots, S_n$ denote the singular arcs in the ribbon. In W there exists a collection of annuli $\{A_1, A_2, \ldots, A_n\}$ with the following properties:

(1) The annuli $\{A_1, A_2, \ldots, A_n\}$ are mutually disjoint.

(2) Each annulus A_i is properly embedded in U.

(3) Each annulus A_i intersects the ribbon transversely in a circle which bounds a disk containing S_i and which misses all other double arcs.

A good deal of flexibility is available in choosing such annuli. To avoid pathologies, however, take each annulus A_i to be as pictured in Fig. 5.

Now, for each i, let $\Sigma_i = A_i \cup c * \mathrm{Bd}(A_i)$. These pinched 2-spheres $\Sigma_1, \Sigma_2, \ldots, \Sigma_n$ serve as placeholders for the 3-cells which are attached to $W \cup c * \mathrm{Bd}(U)$ to complete the description for the ribbon disk complement. In summary, the ribbon disk comple-

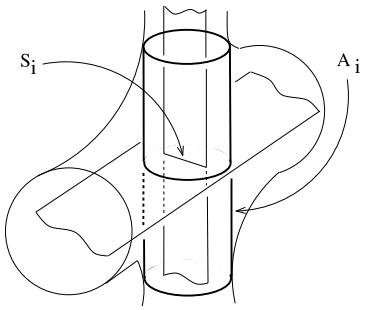

Fig. 5. A typical annulus, A_i, in the collection $\{A_1, A_2, \ldots, A_n\}$.

ment in the 4-ball has the 3-deformation type of the 3-complex

$$W \cup c * \mathrm{Bd}(U) \cup \{D_1, D_2, \ldots, D_n\},$$

where W is a ribbon knot complement in a cube with handles U and each D_i is a 3-cell attached to $W \cup c * \mathrm{Bd}(U)$ along a pinched 2-sphere per the instructions above.

REMARK 2.1. As noted earlier, the motivation for this description for a ribbon disk complement is given in Appendix A. This description will soon be modified and will ultimately be shown, in Appendix B, to be equivalent to the standard LOT description.

REMARK 2.2. It follows from this description that the ribbon disk group is isomorphic to the fundamental group of the 3-complex $W \cup c * \mathrm{Bd}(U)$, a singular 3-manifold with precisely one non-manifold point, its cone point.

REMARK 2.3. By [2, Lemma 2.1], the 3-complex $W \cup c * \mathrm{Bd}(U)$ 3-deforms to the ribbon knot complement in S^3 together with 2-cells attached along a complete set of meridional curves in $\mathrm{Bd}(U)$. It follows that the ribbon disk group is a homomorph of the classical ribbon knot group, a fact which has been observed in the literature. Notice, in this context, the kernel of the epimorphism is normally generated by the meridional curves in $\mathrm{Bd}(U)$.

The current description for the ribbon disk complement permits modifications in several directions. The description, for example, permits collapses which eliminate the 3-cells $\{D_1, D_2, \ldots, D_n\}$. The price for performing these collapses is the addition of spanning arcs to the ribbon knot. This is the content of the following theorem, which serves as the main statement of the alternate description.

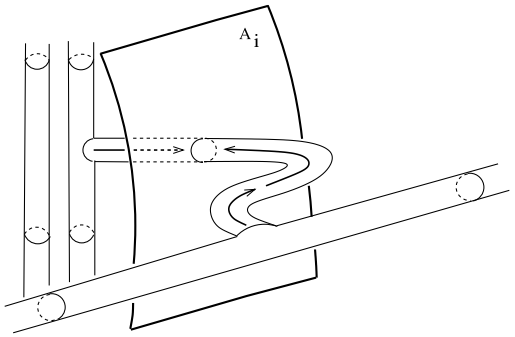

Fig. 6. A typical series of collapses which leads to the removal of a 3-cell D_i.

Theorem 2.1. *A ribbon disk complement can be described as a* 3*-complex of the form*

$$[U \setminus \Gamma] \cup c * \mathrm{Bd}(U),$$

where U *is a* 3*-dimensional cube with handles and* Γ *is an interior graph in* U*. The graph* Γ *contains the original ribbon knot and is obtained by attaching spanning arcs to the ribbon knot, one spanning arc for each ribbon singularity.*

Proof. The main idea for the proof is demonstrated in Fig. 6. In a neighborhood of each singular arc S_i, collapse toward the annulus A_i from either direction, starting at faces on the boundary of a regular neighborhood of the knot. These collapses create a free face in A_i and the 3-cell D_i may now be collapsed through this free face. Performing such a series of collapse for each i achieves the promised modification of the ribbon disk complement.

The reader satisfied with the intuitive argument above may wish to skip ahead to Remark 2.4. A more precise argument for the claim in Theorem 2.1 is made below.

Let $\rho\colon B^2 \to S^3$ denote the ribbon immersion and let $\{S_1, S_2, \ldots, S_n\}$ denote the singular arcs in $\rho(B^2)$. For each i, let $\rho^{-1}(S_i) = \Delta_i \cup \delta_i$, where Δ_i is a large, properly-embedded arc in B^2 and δ_i is a small, interior arc. There exists a collection $\{\alpha_1, \alpha_2, \ldots, \alpha_n\}$ of arcs in B^2 with the following properties:

(1) $\mathrm{Int}(\alpha_i)$ lies in the component of $\mathrm{int}(B^2) \setminus \cup\{\Delta_1, \Delta_2, \ldots, \Delta_n\}$ which contains δ_i.
(2) One endpoint of α_i is an endpoint of δ_i and the other endpoint of α_i lies on $\mathrm{Bd}(B^2)$.
(3) α_i does not meet any peer α_j and does not meet any circle $\rho^{-1}(A_j)$ except $\rho^{-1}(A_i)$, which it meets transversely in a single point.

Fig. 7 demonstrates a choice of arcs α_i for a ribbon with two singularities used in an earlier example. The arcs $\rho(\alpha_i)$ guide the collapses which eliminate the 3-cells D_i.

Without loss of generality, it may be assumed that the description has a CW decomposition such that A_i, $N(\rho(\alpha_i))$, $N(\rho(\alpha_i)) \cap A_i$, and $N(\rho(\alpha_i)) \cap N(\rho(\mathrm{Bd}(B^2)))$ are

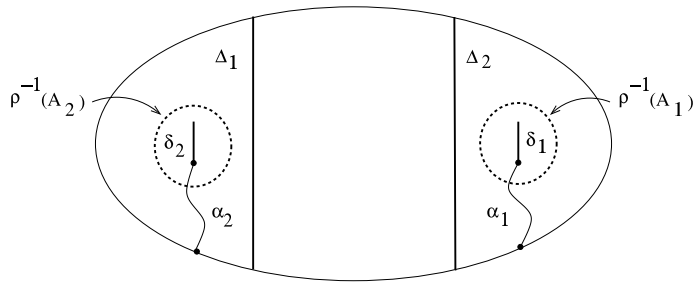

Fig. 7. A choice of arcs $\{\alpha_1, \alpha_2\}$ in B^2 for a ribbon with two singularities. The images of these arcs guide the collapses in the ribbon disk complement.

subcomplexes for each i and the regular neighborhoods $N(\rho(\alpha_i))$ are mutually disjoint. The two 2-cells which comprise $N(\rho(\alpha_i)) \cap N(\rho(\mathrm{Bd}(B^2)))$ are both free faces on $N(\rho(\alpha_i))$. Collapse $N(\rho(\alpha_i))$ through these free faces toward $N(\rho(\alpha_i)) \cap A_i$. The 2-cell $N(\rho(\alpha_i)) \cap A_i$ is now a free face on D_i. Collapse D_i through this free face. Observe the effect of this operation: The 3-cell D_i is now absent and the graph $\rho(\mathrm{Bd}(B^2))$ removed from U has been enlarged by a spanning arc. Continuing in this way all 3-cells $D_1, D_2, \ldots, D_n$ may be removed from the description of the ribbon disk complement. □

REMARK 2.4. For a result similar to Theorem 2.1, the reader is encouraged to see [4, Theorem 3]. There, a strong connection is made between LOT spines and complements of properly embedded arcs in cones over surfaces.

REMARK 2.5. The reader is cautioned not to confuse the terms *core graph* and *ribbon graph*. The term core graph refers to a 1-dimensional core for a thickening of a ribbon. On the other hand, the term ribbon graph refers to a ribbon knot with spanning arcs attached, as in the statement of Theorem 2.1.

EXAMPLE 2.1. To illustrate Theorem 2.1, consider again the example of a ribbon with two singularities. In this case, the ribbon disk complement is described as a ribbon graph complement in a cube with two handles, together with the cone over the boundary of the cube with handles. The ribbon graph is obtained from the original ribbon knot by attaching two spanning arcs, one for each singularity. The outcome is shown in Fig. 8.

At this point, further modifications of the main description are available. One could, for example, aim to remove the cone from the description. This is done in Section 4, where a modified 3-dimensional description is obtained. On the other hand, one could aim to collapse the description to a 2-dimensional complex, from which a presentation for the ribbon disk group can be written. This latter goal will now be pursued.

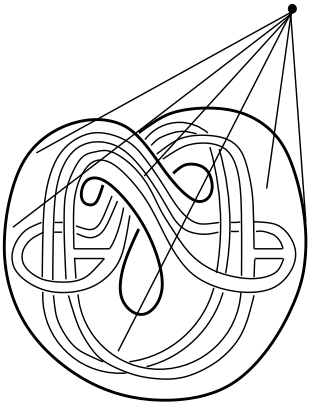

Fig. 8. A ribbon disk complement for a ribbon with two singularities.

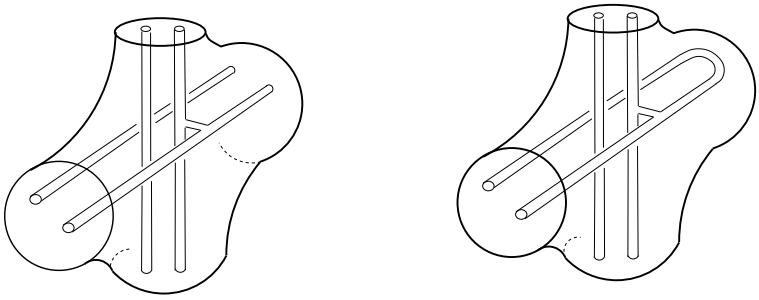

Fig. 9. The two types of hubs: 4-valent and 3-valent.

As before, neighborhoods of the singularities are the primary focus. Each transverse self-intersection in the ribbon creates an area of interest, a *hub*, in the description of the ribbon disk complement. A hub will be called 4-valent or 3-valent, depending on the valence of the corresponding vertex in the core graph. Fig. 9 illustrates the two types of hubs. The key observation is that each type of hub, whether 4-valent or 3-valent, collapses to a 2-complex whose fundamental group is free of rank 2. This reduction to a 2-complex will be shown for a 4-valent hub.

Using Fig. 10 as a guide, begin by partitioning the hub into three sections: a top section, middle section, and bottom section. The top and bottom sections are identical and serve merely as transitions. By comparison, the middle section is the most interesting, as it captures the structure of the hub. Some liberty is taken with the shapes of regions to best illustrate the collapses which follow.

First, collapse the interiors of the sections as completely as possible, preserving exterior walls while doing so. The motive here is to create space in the interiors of

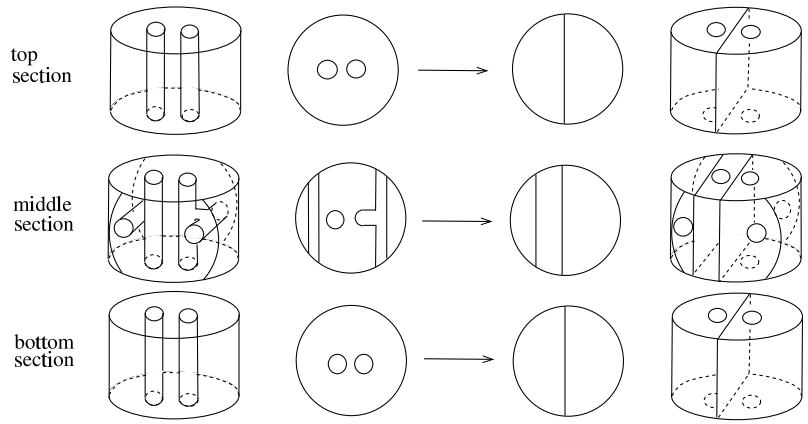

Fig. 10. Interior collapses in the top, middle, and bottom sections (top views included to illustrate collapses).

sections by collapsing toward their exterior walls. It helps to view these collapses from the top, thus this vantage point is taken in Fig. 10. Notice that the exterior walls of the sections are intact after the first stage of collapses.

Next, collapse as completely as possible the horizontal walls which separate the sections. Notice that vertical interior walls created in the first stage restrict collapses of horizontal walls in this second stage. For example, the floor of the top section (which is the same as the ceiling of the middle section) does not collapse completely due to this restriction. Fig. 11 (a) illustrates. Select 2-cells in the figure are shaded to emphasize that they do not collapse. As before, the vertical exterior walls are preserved, to be addressed in the final stage.

Lastly, collapse as completely as possible the vertical exterior walls. Recall that the alternate description for the ribbon disk complement requires a cone over the boundary of the cube with handles. This cone allows much of these walls to collapse. Each section has two exterior 2-cells which are free faces for 3-cells created by the cone. These 2-cells are deleted (to collapse the 3-cells). The middle section may be collapsed a bit further near the four holes in its walls. The cells deleted here are not attached to the cone. Rather, their vicinity to the holes allows them to be deleted. Fig. 11 (b) shows the outcome.

To complete the collapse of the hub, delete all 1-cells which are free faces on 2-cells created by the cone. Then, do the same for 0-cells which are free faces on 1-cells created by the cone. Fig. 11 (c) shows what is left when all such collapses are made. Reconnecting the three pieces, one recovers the 2-complex to which the 4-valent hub collapses. Similarly, a 3-valent hub may be collapsed to a 2-dimensional complex. While verifying, the reader is encouraged to follow the outline above and to take a top view to witness the collapses. Fig. 12 summarizes the findings.

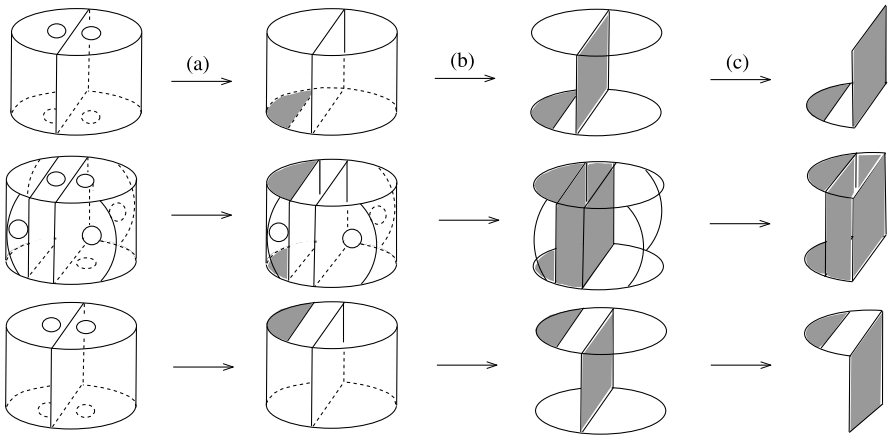

Fig. 11. Collapses in (a) the horizontal walls which separate the sections and then (b) and (c) the vertical exterior walls.

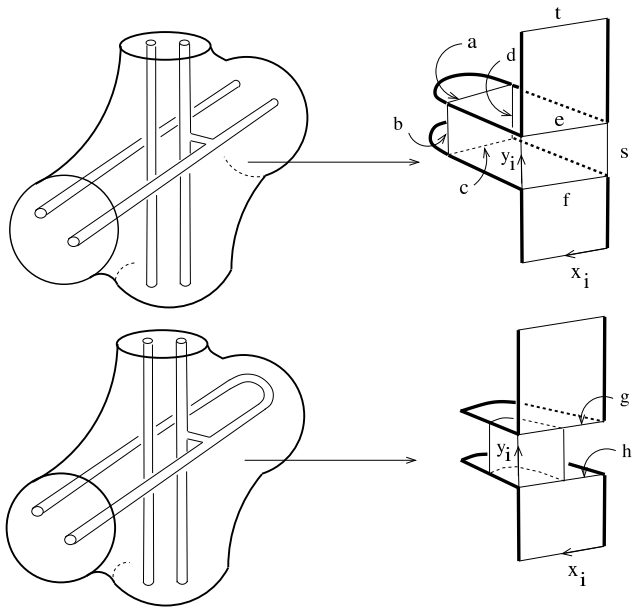

Fig. 12. Collapsing hubs to obtain spines for ribbon disk complements. Recall, on the left a cone is taken over the boundary of the cube with handles. Likewise, on the right a cone is taken over the bold edges in the 2-complexes. (Edges of the 2-complexes are labeled in the figure in anticipation of computing fundamental groups.)

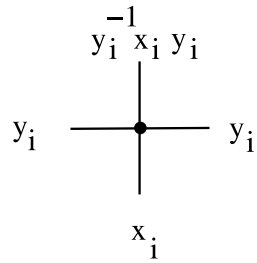

Fig. 13. Labels at a vertex of a core graph. (The two 3-valent vertices in the core graph are labeled similarly, with one of the side edges omitted.)

In both the 4-valent and 3-valent cases, the fundamental group of the reduced 2-complex is a free group on two generators, x_i and y_i. For example, in the case of a 4-valent hub, take the base point to be the cone point and take the maximal tree to be the collection of edges from the cone point to the vertices. Assume that all horizontal edges agree in orientation with x_i and that all vertical edges agree in orientation with y_i. A presentation for the 2-complex then becomes

$$\{a, b, c, d, e, f, s, t, x_i, y_i \mid te^{-1}, a, c, b^{-1}y_i, ab^{-1}c^{-1}d, d^{-1}s, ey_i^{-1}f^{-1}s, fx_i^{-1}\},$$

which reduces to $\{x_i, y_i \mid \}$ by extended Nielsen operations. Furthermore, under this reduction, the side edge s corresponds to y_i and the top edge t corresponds to $y_i^{-1}x_iy_i$. Likewise, it is seen for the case of a 3-valent hub that the fundamental group of the 2-complex is free on the generators x_i, y_i. Here, too, the side edge s corresponds to y_i and the top edge t corresponds to $y_i^{-1}x_iy_i$. For this calculation, take the cone point as the base point and include all edges from the cone point to the vertices in the maximal tree, as before. In this case, however, additional edges need to be included to make the tree maximal. The edges g and h suffice.

A 2-dimensional spine for the ribbon disk complement, therefore, may be described as a union of collapsed hubs, connected via their top, bottom, and side edges. The core graph documents the connections to be made. Altogether, this suggests an algorithm for writing a geometric presentation for the ribbon disk group.

ALGORITHM 1 for writing a presentation for a ribbon disk group. First, place distinct labels on the vertices of the core graph as shown in Fig. 13.

Then:

(1) For each vertex of the core graph, one writes two generators, x_i and y_i.

(2) For each edge of the core graph with labels, say, l_1 and l_2 on its ends, one writes a relator of the form $l_1 = l_2$ or $l_1 = l_2^{-1}$, depending on whether the hubs are connected without or with a half-twist.

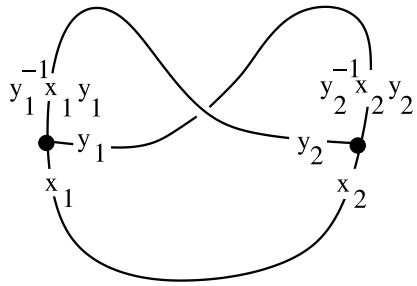

Fig. 14. A presentation for the ribbon disk group: $\{x_1, x_2, y_1, y_2 \mid x_1 = x_2^{-1}, y_1^{-1} = y_2^{-1}x_2y_2, y_1^{-1}x_1y_1 = y_2\}$.

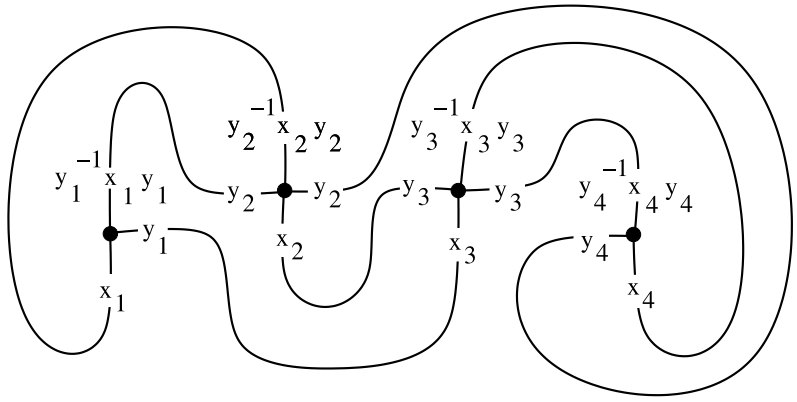

Fig. 15. A presentation for the ribbon disk group: $\{x_1, x_2, x_3, x_4, y_1, y_2, y_3, y_4 \mid x_1 = y_2^{-1}x_2y_2, y_1 = x_3, y_1^{-1}x_1y_1 = y_2, x_2 = y_3, y_2 = y_4, y_3 = y_4^{-1}x_4y_4, y_3^{-1}x_3y_3 = x_4\}$.

EXAMPLE 2.2. To demonstrate the algorithm for obtaining a ribbon disk group presentation, an earlier example of a ribbon with two singularities is revisited. Its core graph, with labels, is drawn in Fig. 14, and the presentation for its ribbon disk group is written below. The presentation has 4 generators (two for each vertex) and 3 relators (one for each edge). The first relator, $x_1 = x_2^{-1}$, documents that the bottom of hub 1 is attached to the bottom of hub 2, with a half-twist.

EXAMPLE 2.3. A second, more sophisticated core graph is shown in Fig. 15. Assume that its connections are made without half-twists. The presentation for this ribbon disk group has 8 generators and 7 relators, corresponding to the 4 vertices and 7 edges in the core graph. The first relator, $x_1 = y_2^{-1}x_2y_2$, documents that the bottom of hub 1 is connected to the top of hub 2.

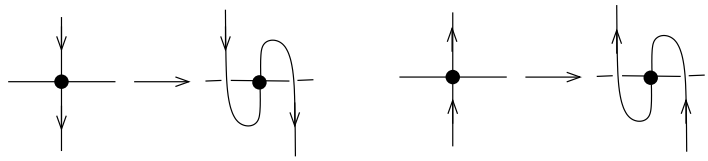

Fig. 16. Local changes at a vertex of the core graph to remove a half-twist. On the left, the path P originally traverses the vertex top-to-bottom. It is made to traverse the vertex bottom-to-top instead, altering P only in a neighborhood of the vertex. Likewise, on the right, a bottom-to-top traverse is switched to a top-to-bottom traverse by altering P locally.

REMARK 2.6. A core graph without twisted connections will be said to be *twist-free*. Relators given by a twist-free core graph read $x_i = x_j$ or $y_i = y_j^{-1}x_j y_j$, for example, and not $x_i = x_j^{-1}$ or $y_i = (y_j^{-1}x_j y_j)^{-1}$. Any core graph with twists can be replaced by a twist-free core graph without changing the homotopy type of the corresponding 2-complex. Put another way, a ribbon with twists can be replaced by a ribbon without twists without changing the homotopy type of the complement. This follows, intuitively, from the fact that the homotopy type of the complement is determined by its LOT. Beneficial, local changes can be made to a ribbon without changing the LOT. This claim for core graphs is justified, formally, below.

It suffices to show that any core graph with half-twists can be replaced by a core graph with fewer half-twists. Recall it is assumed that the core graph has two vertices of valence 3 and remaining vertices of valence 4. Each vertex has a top edge and a bottom edge incident to it, and either one or two side edges incident to it, depending on its valence. There exists in the core graph a path P (unique up to orientation) which begins at the side edge of one 3-valent vertex, ends at the side edge of the other 3-valent vertex, and moves transversely through the remaining 4-valent vertices. That is, P moves top-to-bottom, bottom-to-top, or side-to-side through each vertex, mimicking on the page the formation of the ribbon in space. Notice P includes each vertex of the core graph twice and each edge once. Following P, label its initial vertex 1, the next vertex traversed side-to-side 2, the next vertex traversed side-to-side 3, and so on. Thus, the vertices are numbered $1, 2, \ldots, n$ as they are traversed side-to-side. Let $[1, 2], [2, 3], \ldots, [n, n-1]$ denote the corresponding subpaths of P.

Now, suppose the core graph has a half-twist, witnessed by an edge e. Then e is in subpath $[i, i+1]$ for some i $(1 \leq i \leq n-1)$. The core graph is altered as follows:
(1) For each vertex $k \geq i+1$, interchange its top and bottom connections. As Fig. 16 illustrates, interchanging the top and bottom connections is a local move on P which leaves other connecting data unchanged.
(2) Remove the half-twist witnessed by edge e.

It is claimed that the presentations associated with the original and new core graphs are Nielsen equivalent. The following Nielsen moves on the original presentation achieve this equivalence:
(1) $x_k \to y_k x_k y_k^{-1}$ for $k \geq i+1$,
(2) $y_k \to y_k^{-1}$ for $k \geq i+1$,
(3) $x_j \to x_j^{-1}$ for each vertex j traversed top-to-bottom or bottom-to-top by subpath $[i, i+1] \cup \cdots \cup [n-1, n]$.
Notice that moves of type (1) and (2) switch the top and bottom labels at a vertex:
(top label) $y_k^{-1} x_k y_k \to x_k$,
(bottom label) $x_k \to y_k x_k y_k^{-1} \to y_k^{-1} x_k y_k$.
This agrees with the local change in the core graph at such a vertex. Further, notice that moves of type (3) assure that the old connecting data is preserved (except, of course, for the one edge on which it is changed). In particular, consider any edge in the core graph besides the edge e. Then P traverses this edge either before or after it traverses e. If before, then both labels on this edge are unchanged and the connecting data is preserved. If after, then both labels on this edge are changed to their inverses, again preserving the connecting data. For the edge e itself, one of its labels is necessarily changed to its inverse and the other is not, removing the half-twist from the connecting data. This completes the formal proof of the claim made in Remark 2.6.

3. Asphericity results using graph-theoretic criteria

The first application of the alternate description is a graph-theoretic result in the spirit of [7, Theorem 10.1], which states that a ribbon disk complement is aspherical provided a certain graph kindred to the LOT is a tree. A slightly generalized version of this result will actually be used here. Consider a group presentation of the form $\mathcal{P} = \{x_1, x_2, \ldots, x_m \mid a_1 = b_1, a_2 = b_2, \ldots\}$, where a_j, b_j, $j = 1, 2, \ldots$ are nonempty words in the alphabet $\{x_1^+, x_2^+, \ldots, x_m^+\}$ and the words $a_j b_j^{-1}$ are cyclically reduced. The *right graph* of $\mathcal{P}$, $\Phi(\mathcal{P})$, is defined to be the graph on vertices $x_1, x_2, \ldots, x_m$ whose edges e_j are in one-to-one correspondence with the relators $a_j = b_j$ such that e_j connects x_{j_1} and x_{j_2} provided a_j, b_j end in x_{j_1}, x_{j_2} respectively. It is known that if $\Phi(\mathcal{P})$ is a forest, then the 2-complex modeled on $\mathcal{P}$ is aspherical ([10] and [12]). This result is the main observation in the proof of the following theorem.

Theorem 3.1. *Suppose all edges containing a bottom label are deleted from a twist-free core graph. If the graph which remains is a forest, then the ribbon disk complement is aspherical.*

Proof. Let $\mathcal{P}$ denote the presentation based on the core graph and let $\Phi(\mathcal{P})$ denote its right graph. It suffices to show that $\Phi(\mathcal{P})$ is a forest. Recall that the relators in $\mathcal{P}$ correspond to the edges in the core graph. If, for example, an edge in the core graph has two bottom labels, then the corresponding relator in $\mathcal{P}$ is of the form

$x_i = x_j$. In $\Phi(\mathcal{P})$, one gets an edge joining x_i and x_j. If an edge in the core graph has one top label and one bottom label, then the corresponding relator in $\mathcal{P}$ is of the form $x_i = y_j^{-1}x_j y_j$, or $y_j x_i = x_j y_j$. In this case, one gets an edge in $\Phi(\mathcal{P})$ joining x_i and y_j. Technically, the relator $y_i^{-1}x_i y_i = y_j^{-1}x_j y_j$ is faulty as it has negative powers and these negatives cannot be voided by simply moving letters to opposite sides. This issue may be resolved, however, by an elementary expansion of $\mathcal{P}$. For each such relator, add to $\mathcal{P}$ a new generator t and a new relator $t = y_i^{-1}x_i y_i$. This new relator is of an appropriate type, as it can be rewritten $y_i t = x_i y_i$. The old relator may now be rewritten as $t = y_j^{-1}x_j y_j$, or $y_j t = x_j y_j$, making it appropriate as well. In $\Phi(\mathcal{P})$, an edge connects y_i to t and another connects t to y_j. Since no other edges in $\Phi(\mathcal{P})$ meet t, the two edges may be regarded as a single edge in $\Phi(\mathcal{P})$ connecting y_i and y_j. An analysis of remaining cases fills in the table below.

edge in core graph	relator	edge in $\Phi(\mathcal{P})$
bottom-bottom	$x_i = x_j$	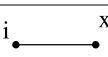
bottom-side bottom-top	$x_i = y_j$ $x_i = y_j^{-1}x_j y_j$	
side-side side-top top-top	$y_i = y_j$ $y_i = y_j^{-1}x_j y_j$ $y_i^{-1}x_i y_i = y_j^{-1}x_j y_j$	

The proof of the theorem is completed by observing that each vertex x_i in $\Phi(\mathcal{P})$ has valence 1. The bottom of hub i makes one connection and this connection produces the one edge in $\Phi(\mathcal{P})$ incident to x_i. No other connection produces an edge incident to x_i. It follows that any cycle in $\Phi(\mathcal{P})$ must go solely through y vertices. Such a cycle exists in $\Phi(\mathcal{P})$, however, only if there is a corresponding cycle in the core graph consisting solely of top and side connections. By assumption, no such cycle exists. □

EXAMPLE 3.1. The core graph in Fig. 17, for example, satisfies the graph-theoretic criterion of Theorem 3.1. The corresponding ribbon disk complement is therefore aspherical. Edges with bottom labels are given a lighter weight, to emphasize the application of the criterion. Notice that deleting the lighter edges leaves a tree.

The geometric nature of the alternate description for a ribbon disk complement will continue to be utilized. The next goal is to express a ribbon disk complement as a union of aspherical spaces whose intersection is aspherical and π_1-injective. This requires that the intersection be simple relative to the spaces and is accomplished by requiring a certain cut-edge property in the core graph.

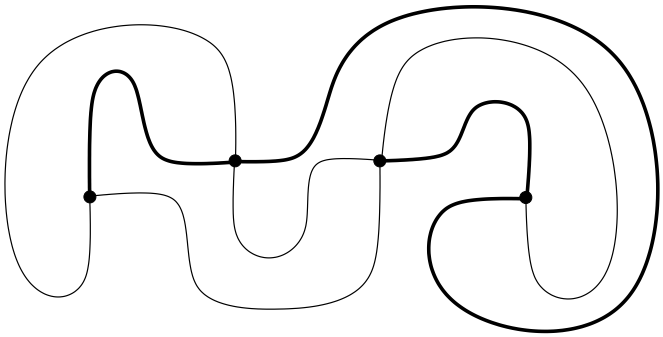

Fig. 17. Example of a core graph which satisfies the graph-theoretic criterion of Theorem 3.1.

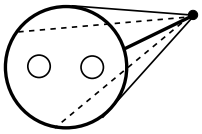

Fig. 18. $Y_1 \cap Y_2$ is a sphere with two holes, which has the homotopy type of a circle.

Theorem 3.2. *Suppose a core graph C can be written as $C = A \cup e \cup B$, where A, B are disjoint core graphs and e is an edge which connects them. If A and B correspond to aspherical ribbon disk complements, then C corresponds to an aspherical ribbon disk complement.*

Proof. Using Theorem 2.1, let Y denote the description of the ribbon disk complement which corresponds to C. Recall that Y is a ribbon graph complement in a cube with handles U together with the cone over $\mathrm{Bd}(U)$. By hypothesis, U consists of two disjoint cubes with handles (corresponding to graphs A, B) connected with a 1-handle E (corresponding to the edge e). A transverse disk in E essentially splits Y, suggesting a natural decomposition of Y. Taking this suggestion, write Y as a union, $Y = Y_1 \cup Y_2$, such that:

(1) $Y_1 \cap Y_2$ has the homotopy type of a circle (Fig. 18); and
(2) Y_1, Y_2 have the homotopy types of aspherical ribbon disk complements.

The first property follows from the fact that $Y_1 \cap Y_2$ is a sphere with two holes. Notice that a transverse disk in E meets the ribbon graph in two points. The two holes in this disk correspond to these points of intersection. Meanwhile, the cone over the boundary of the disk is required by the description of the ribbon disk complement. The second property follows from the fact that Y_1, Y_2 correspond to the graphs A, B, which are assumed to be core graphs for aspherical ribbon disk complements.

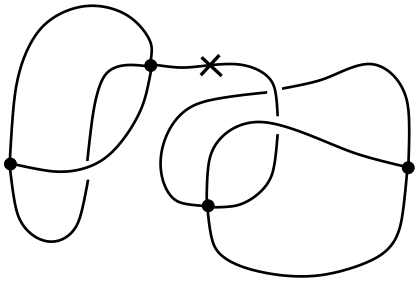

Fig. 19. Example of a core graph which satisfies the criterion of Theorem 3.2, with cut-edge marked.

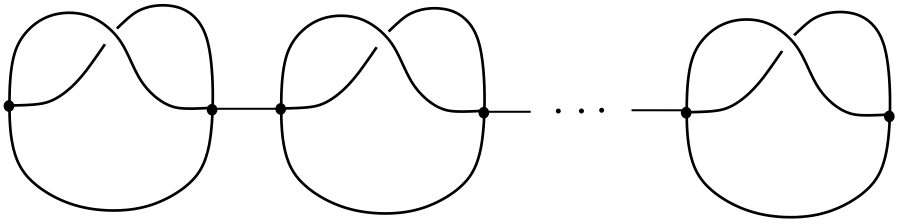

Fig. 20. A core graph whose corresponding ribbon disk complement is known, inductively, to be aspherical.

Now, $Y_1 \cap Y_2$ is aspherical, as it has the homotopy type of a circle. Further, the generator for $\pi_1(Y_1 \cap Y_2)$ maps to nontrivial elements in the torsion-free groups $\pi_1(Y_1)$ and $\pi_1(Y_2)$. It follows that $\pi_1(Y_1 \cap Y_2)$ injects into $\pi_1(Y_1)$ and $\pi_1(Y_2)$. By [13, Theorem 5], Y is aspherical. □

REMARK 3.1. A strong connection has been established between the group-theoretic property of *local indicability* and the topological property of asphericity [5]. The result in Theorem 3.2 may be viewed as a topological analog of the fact that the amalgamated product of locally indicable groups via infinite cyclic subgroups is itself locally indicable [8, Theorem 9]. Recall that the intersection space used in the proof of Theorem 3.2 has the homotopy type of a circle. Amalgamating two aspherical spaces along this intersection space gives an aspherical space.

EXAMPLE 3.2. The core graph in Fig. 19 satisfies the criterion of Theorem 3.2. Deleting the marked cut-edge produces two valid core graphs. These subgraphs are known to correspond to aspherical ribbon disk complements, as the LOT's for their ribbons have diameters less than or equal to 3 [7, Theorem A].

EXAMPLE 3.3. Inductively, families of ribbons with increasing diameters can be formed whose complements are known to be aspherical. Fig. 20 suggests how to proceed.

4. An asphericity result using a relative homotopy group

The description for the ribbon disk complement in Theorem 2.1 allows for modifications in different directions. Rather than collapsing to a 2-dimensional complex, one may wish instead to remove the cone from the description. To this end, [2, Lemma 2.1] applies. It is known that the description in Theorem 2.1 3-deforms to the ribbon graph complement $S^3 \setminus \Gamma$ with 2-cells attached along a complete set of meridional curves in $\mathrm{Bd}(U)$. A modification in this direction yields a second algorithm for writing a presentation for a ribbon disk group. In this case the presentation is written as a relative presentation $\{\mathcal{W} \mid \mathcal{R}\}$ with respect to a standard Wirtinger presentation $\mathcal{W}$ for the ribbon graph group.

ALGORITHM 2 for writing a presentation for a ribbon disk group. First, draw a ribbon graph Γ which corresponds to the ribbon. To avoid pathologies, use the method in the proof of Theorem 2.1 to obtain the ribbon graph. Next, identify a complete set of meridional disks in a thickening of the ribbon. A complete set of transverse disks suffices.

Then:

(1) Write the standard Wirtinger presentation, $\mathcal{W}$, for the graph group $\pi_1(S^3 \setminus \Gamma)$.
(2) Add to $\mathcal{W}$ one relator for each meridional disk in the collection above. Each such relator is of the form $x_i x_j^{-1}$ for some generators x_i, x_j in $\mathcal{W}$ and denotes the word in $\pi_1(S^3 \setminus \Gamma)$ read by the boundary of the meridional disk. The nature of the ribbon ensures that each relative relator has length two.

Fig. 21 illustrates the modified description for the ribbon disk complement using the example of a 2-singularity ribbon considered earlier. The ribbon disk complement can be described as $[S^3 \setminus \Gamma] \cup \{E_1, E_2\}$, where Γ is the ribbon graph and E_1, E_2 are the 2-cells shown in Fig. 21. These 2-cells form a complete set of meridional disks in a thickening of the ribbon. The corresponding ribbon disk group has a presentation of the form $\{\mathcal{W} \mid x_i x_j^{-1}, x_m x_n^{-1}\}$, where $\mathcal{W}$ is a standard Wirtinger presentation for the ribbon graph group and the x's are generators in that presentation.

The current description for ribbon disk complements suggests a natural pair of spaces to consider: the ribbon disk complement itself and the ribbon graph complement which is a subspace of it. Graph complements in S^3 are well-studied 3-manifolds whose properties lead to the next asphericity result.

Theorem 4.1. *Let $Y = [S^3 \setminus \Gamma] \cup \{E_1, E_2, \ldots, E_n\}$ denote the ribbon disk complement as described above and let X be the subspace $S^3 \setminus \Gamma$. If $\pi_2(Y, X)$ is a free group, then Y is aspherical.*

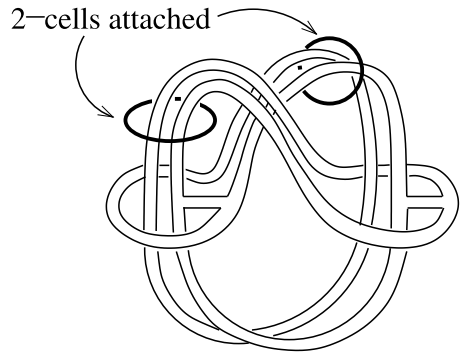

Fig. 21. A modified 3-dimensional description for the ribbon disk complement. The cone is removed from the earlier description, replaced by two 2-cells attached along meridional curves in a thickening of the ribbon.

Proof. Noting that $\pi_2(X) = 0$, the long exact sequence of the pair (Y, X) gives:

$$0 \to \pi_2(Y) \to \pi_2(Y, X) \xrightarrow{\partial} \pi_1(X) \to \pi_1(Y) \to 0.$$

Now, $\mathrm{rk}(\pi_2(Y, X)) \geq 1$ must be true, as it is a free crossed module over $\pi_1(X)$ with boundary map ∂ and a basis which corresponds to $\{E_1, E_2, \ldots, E_n\}$ ([14]).

If $\mathrm{rk}(\pi_2(Y, X)) = 1$, i.e. $\pi_2(Y, X) \cong \mathbb{Z}$, then ∂ is either the zero map or is one-to-one. (Note that $\pi_1(X)$ is torsion-free.) However, ∂ cannot be the zero map. On one hand, $\partial \equiv 0$ implies $\pi_2(Y) \cong \pi_2(Y, X) \cong \mathbb{Z}$. On the other hand, $\partial \equiv 0$ implies $\pi_1(Y) \cong \pi_1(X)$. Since X is an irreducible 3-manifold with boundary, the group $\pi_1(X)$ is locally indicable [5, Corollary 6.2]. It follows by [5, Theorem 5.2] that $\pi_2(Y) = 0$, contradicting an earlier consequence. It must be true, therefore, that ∂ is one-to-one. By exactness, $\pi_2(Y) = 0$, as desired.

If $\mathrm{rk}(\pi_2(Y, X)) > 1$, then the center of $\pi_2(Y, X)$ is trivial. However, $\ker \partial$ is contained in the center of $\pi_2(Y, X)$ [9, Section 1], and thus $\ker \partial = 0$. Again, by exactness, $\pi_2(Y) = 0$. □

Corollary 4.1. *If the graph Γ is Heegaard in S^3, then Y is aspherical if and only if $\pi_2(Y, X)$ is a free group.*

Proof. If $\pi_2(Y, X)$ is a free group, then $\pi_2(Y) = 0$ by Theorem 4.1, whether Γ is Heegaard or not. On the other hand, suppose Γ is Heegaard and $\pi_2(Y) = 0$. Consider again the exact sequence of the pair (Y, X):

$$0 \to \pi_2(Y) \to \pi_2(Y, X) \xrightarrow{\partial} \pi_1(X) \to \pi_1(Y) \to 0.$$

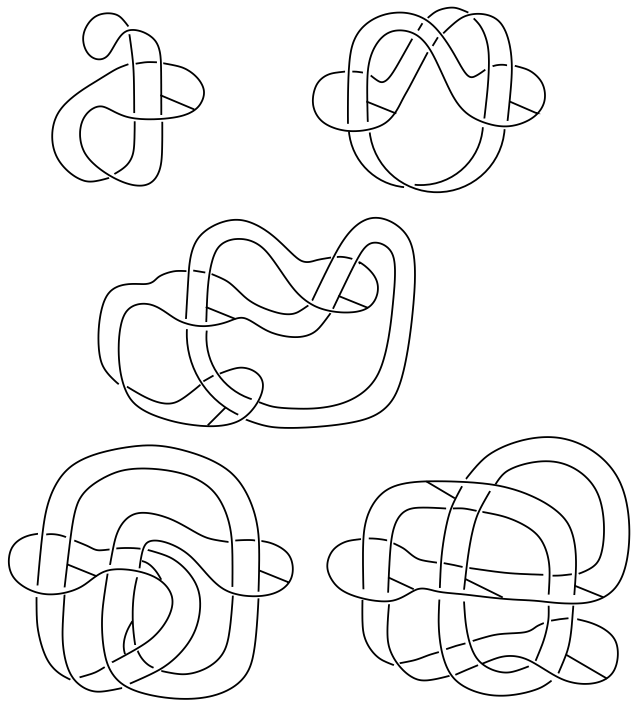

Fig. 22. Several ribbon graphs known to be Heegaard.

Note that $\pi_2(Y, X)$ injects into $\pi_1(X)$, which is a free group by hypothesis. Therefore, $\pi_2(Y, X)$ is itself free by the Nielsen–Schreier theorem. □

REMARK 4.1. The ribbon graph associated with a ribbon may indeed be Heegaard. In fact, ribbons which yield Heegaard ribbon graphs seem to form a sizable subset of all ribbons. The ribbon graphs in Fig. 22, for example, are all Heegaard. For each of these graphs, the group of the graph complement in S^3 is free.

REMARK 4.2. Not all ribbon graphs are Heegaard, however. The ribbon graph in Fig. 23, for example, is not. In this example, $\pi_1(S^3 \setminus \Gamma) = \langle a, b, x, y \mid abab^{-1}a^{-1}b^{-1} \rangle$, which is not a free group, as it contains the trefoil group $\langle a, b \mid abab^{-1}a^{-1}b^{-1} \rangle$ as a free factor. Interestingly, the ribbon disk complement in this example has the homotopy type of the classical trefoil knot complement.

A. Motivation for the initial description of the ribbon disk complement

Motivation for the initial description given in Section 2 progresses in two stages. First, the ribbon is moved along the fibers of a collar of $S^3 = \mathrm{Bd}(B^4)$ such that the ribbon knot remains in $\mathrm{Bd}(B^4)$ and the rest of the ribbon moves to its interior. The

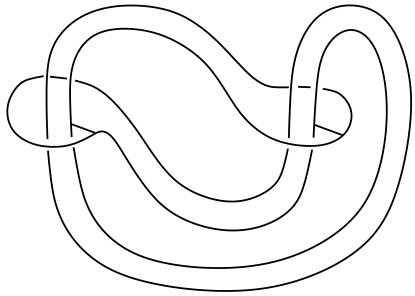

Fig. 23. Example of a ribbon graph which is not Heegaard.

ribbon continues to be a singular disk in the initial stage and an intermediate spine for the complement is described. In the second stage, the singularities in the ribbon are resolved by applying 3-deformations and then deleting residual arcs. It is observed that this resolution causes 3-cells to be added to the intermediate spine.

As before, let U be a regular neighborhood of a ribbon $\mathcal{R} = \rho(B^2)$ in S^3 and let W be the 3-manifold defined by $W = U \setminus \mathring{N}(k)$, where k denotes the ribbon knot. It may be assumed that U is Heegaard, in which case W is a knot complement in an unkotted cube with handles. Let $\mu\colon S^3 \times [0, 1] \to B^4$ be a collar on $\mathrm{Bd}(B^4)$ and let $h_0\colon S^3 \to [0, 1]$ be a continuous height function such that $h_0^{-1}(1) = S^3 \setminus \mathrm{Int}(U)$ and $h_0^{-1}(0) = k$. Define a map h from S^3 into the collar $\mu(S^3 \times [0, 1])$ by $x \to \mu((x, h_0(x))$ and move the ribbon $\mathcal{R}$ to its image $h(\mathcal{R})$ along the fibers of the collar. At this moment, the ribbon resides in the interior of B^4, with the exception of k, which remains in $\mathrm{Bd}(B^4)$.

Define a second height function $h_1\colon S^3 \to [0, 1]$ such that $h_1(x) \leq h_0(x)$ for all $x \in S^3$, and $h_1(x) = h_0(x)$ if and only if $x \in k \cup (S^3 \setminus \mathrm{Int}(U))$. Notice that the 4-manifold $N = \{\mu(u, t) \in B^4 \mid u \in U \text{ and } h_1(u) \leq t \leq 1\}$ is a regular neighborhood of $h(\mathcal{R})$ in B^4. The closure of the complement of N in B^4 consists of three pieces:

$$X_0 = B^4 \setminus \mu(S^3 \times [0, 1)),$$
$$X_1 = \mu((S^3 \setminus \mathrm{Int}(U)) \times [0, 1]),$$

and

$$X_2 = \{\mu(x, t) \in B^4 \mid x \in W \text{ and } 0 \leq t \leq h_1(x)\}.$$

For convenience, label the subspaces $Y_1 = \mu(\mathrm{Bd}(U) \times [0, 1])$ and $Y_2 = \{\mu(x, h_1(x)) \mid x \in W\}$ of the complement. The diagram in Fig. 24 helps identify some of the key spaces in this description.

Now, the the complement $B^4 \setminus N$ collapses to $Y_2 \cup X_0$ by the following sequence of moves:

(1) Collapse X_1 to $Y_1 \cup (X_1 \cap X_0)$.

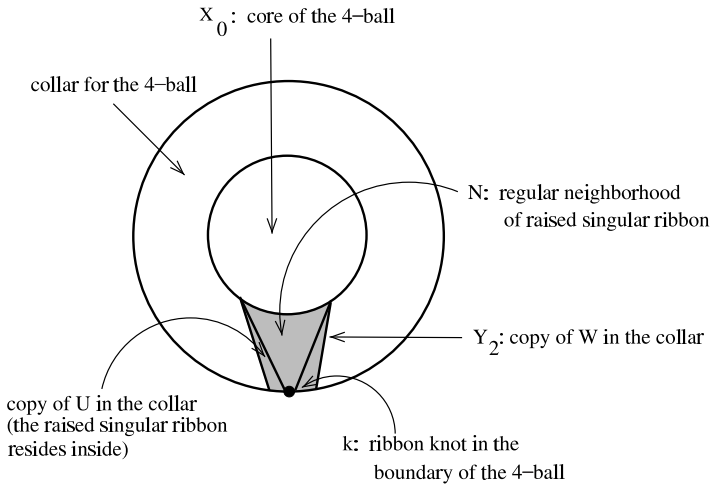

Fig. 24. Key spaces in the description of the complement at an intermediate stage.

(2) Collapse X_2 to Y_2.
(3) Collapse Y_1 to $Y_1 \cap X_0$.

Therefore, at this intermediate stage, the complement has a description homeomorphic to the identification space

$$Y_2 \amalg X_0,$$

where Y_2 and X_0 are identified along the shared space $\{\mu(x, h_1(x)) \mid x \in \mathrm{Bd}(U)\}$. However, Y_2, X_0, and $\{\mu(x, h_1(x)) \mid x \in \mathrm{Bd}(U)\}$ are merely homeomorphic copies of W, B^4, and $\mathrm{Bd}(U)$ respectively. Thus, the identification space may be regarded as

$$W \amalg B^4,$$

where the identification is made along copies of $\mathrm{Bd}(U)$ in the boundaries of W and B^4. Regarding B^4 as the cone $c * S^3$ over its boundary, the space above in turn collapses to the identification space

$$(\dagger) \qquad W \amalg c * \mathrm{Bd}(U),$$

with identifications, again, along copies of $\mathrm{Bd}(U)$. This completes the first stage of the process.

Next, the ribbon's singularities will be resolved. This will nearly be accomplished by way of 3-deformations. Recall that the singular set for the ribbon immersion ρ is a collection of arcs $\{\Delta_i, \delta_i\}$ in B^2 such that the arcs Δ_i separate the interior of B^2 into disjoint open 2-cells. Let C denote a component of $B^2 \setminus \{\Delta_i\}$. For each δ_j

in C, choose an arc α_j in C which connects $\mathrm{Bd}(\delta_j)$ to $\mathrm{Bd}(B^2)$. This process should mimic the method in the proof of Theorem 2.1. (See Fig. 7 for an example.) Then $\mathrm{Int}(C) \setminus \{\delta_j, \alpha_j\}$ is an open 2-cell whose image under ρ is an open 2-cell, say $\hat{C}$, in $\mathcal{R}$. The 2-cell $\hat{C}$ serves as a base for a vertical 3-deformation of the ribbon along the fibers of the collar on $\mathrm{Bd}(B^4)$. Attach a 3-cell along $\hat{C}$ and then collapse immediately through $\hat{C}$. This operation elevates the points of $\mathrm{Cl}(\hat{C})$ in the collar, eliminating the singularities which correspond to the δ_j's. However, a 2-cell with edge $\rho(\delta_j \cup \alpha_j)$ is a byproduct of this move. Perform a side collapse to eliminate the interior of this 2-cell. Each such collapse produces a residual arc, $\rho(\alpha_j)$. Operate in a similar manner on the remaining components of $B^2 \setminus \{\Delta_i\}$ to obtain an embedded ribbon disk in B^4 with residual arcs attached. The complement of this complex has the same deformation type as (†), since it is obtained by perfoming 3-deformations in B^4 on the ribbon. Now, deleting the residual arcs yields the embedded ribbon disk itself. By duality, deleting 1-cells from the complex corresponds to adding 3-cells to its complement. These dual 3-cells complete the description of the ribbon disk complement given at the beginning of Section 2.

B. Equivalence with the standard LOT description

It will be shown that the description for ribbon disk complements used in this work is equivalent to the standard LOT description, up to 3-deformation. In particular, it will be shown that the corresponding presentations are Nielsen equivalent. The presence of the conjugating relators in Algorithm 1 and the fact that the core graph is an immersion of the LOT help make this a reasonable assertion. For the reader's benefit, first a review of the LOT description is given.

As before, let $\rho\colon B^2 \to S^3$ be a ribbon immersion and let $\{S_i\}$, $i = 1, 2, \ldots, n$, denote the double arcs in the ribbon $\rho(B^2)$. For each i, let $\rho^{-1}(S_i) = \Delta_i \cup \delta_i$, where Δ_i is a large, properly-embedded arc in B^2 and δ_i is a small, interior arc. The LOT associated with the ribbon is a tree in B^2 defined by the properties which follow.

Vertices: The vertices of the LOT are in one-to-one correspondence with the components of $B^2 \setminus \{\Delta_i\}$.

Edges: Two vertices are joined by an edge if the corresponding components of $B^2 \setminus \{\Delta_i\}$ share on their boundaries a large arc Δ_j for some j.

Labels: Each edge e of the LOT is labeled with a vertex $\lambda(e)$. If the edge exists by way of a large arc Δ_j, then $\lambda(e)$ is the vertex which corresponds to the component of $B^2 \setminus \{\Delta_i\}$ containing the small arc δ_j.

Orientations: The ribbon $\rho(B^2)$ inherits a positive side and a negative side from the disk B^2. Orient each edge of the LOT such that its image under ρ pierces the ribbon from its negative side.

The LOT spine for the ribbon disk complement is then the 2-complex modeled on the presentation $\{\{v\}_{v\in V} \mid \{\lambda(e)^{-1}\iota(e)\lambda(e)\tau(e)^{-1}\}_{e\in E}\}$, where V, E denote the vertex and edges sets of the LOT and ι, τ help denote initial and terminal vertices of edges.

Regarding the alternate description in this article, one begins with a core graph for the ribbon. By Remark 2.6, it may be assumed that the core graph is twist-free. It is again beneficial to identify a path in the core graph which begins at the side edge of one 3-valent vertex, ends at the side edge of the other 3-valent vertex, and moves transversely through the remaining 4-valent vertices. Recall that such a path traverses each edge exactly once and moves top-to-bottom, bottom-to-top, or side-to-side through each vertex as it does so. Using this path, the core graph can be divided into segments as follows: Segment 1 begins at the initial vertex and ends at the first vertex met at the top or bottom. Segment 2 begins where segment 1 ends and continues until a vertex is met at the top or bottom. Continuing in this way, the core graph can be written as a union of segments which share vertices but do not share edges. Notice that the segments are in one-to-one correspondence with the components of $B^2 \setminus \{\Delta_i\}$.

The core graph yields a group presentation (see Algorithm 1) and the segments of the core graph may be associated with strings of relators in this presentation. Indeed, one may write relators in the order that corresponding edges are traversed, to make the association of segments and strings of relators more clear. A typical string of relators begins and ends with a top or bottom label and has only side labels in between. The first (resp. last) string is exceptional in that it necessarily begins (resp. ends) with a side label. Now, this group presentation may be expanded as follows:

(1) For each segment of length 1 of the form $x_i = x_j$ or $x_i = y_j^{-1} x_j y_j$, add a new generator a and a new relator $a = x_i$.

(2) For each segment of length 1 of the form $y_i^{-1} x_i y_i = y_j^{-1} x_j y_j$, add a new generator a and a new relator $a = y_i^{-1} x_i y_i$.

(3) For each remaining segment, add a new generator a. If the segment contains a bottom label x_i, then add the relator $a = x_i$. If it does not, then it must contain a side label y_i, in which case the relator $a = y_i$ is added. This assignment need not be unique.

This expanded presentation collapses to a presentation on the letters $\{a_j\}$. To achieve this rewriting, first collapse all relators of length 2 by way of (1) and (3) above. Then finish the rewriting by way of (2). The claim is that the new presentation is precisely the LOT presentation for the ribbon disk complement. This is established by making two observations about the presentation, one about its generators and the other about its relators.

Generators in the collapsed presentation. The generators in the collapsed presentation correspond with the segments in the core graph. The segments, in turn, correspond with the components of $B^2 \setminus \{\Delta_i\}$. Therefore, the number of generators is in agreement.

Relators in the collapsed presentation. Only relators involving top labels remain in the collapsed presentation. That is, all relators are now of the form $a_i^{-1} a_j a_i = a_k$. Furthermore, the letters a_j, a_k correspond to consecutive segments. This is true since top labels are conjugates of bottom labels per Algorithm 1. These consecutive segments correspond to components of $B^2 \setminus \{\Delta_i\}$ which share a large singular arc on their boundaries. On the other hand, the conjugating letter a_i corresponds to a segment which meets the vertex at the side. Such a segment corresponds, in turn, to the component

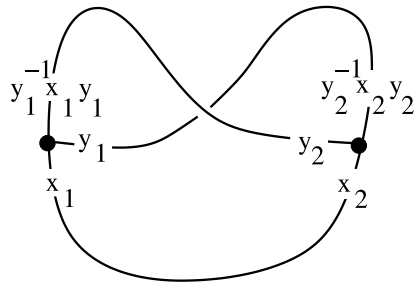

Fig. 25. A core graph from an earlier example. (Note: The twist-free replacement is the same core graph, which does not happen in general.)

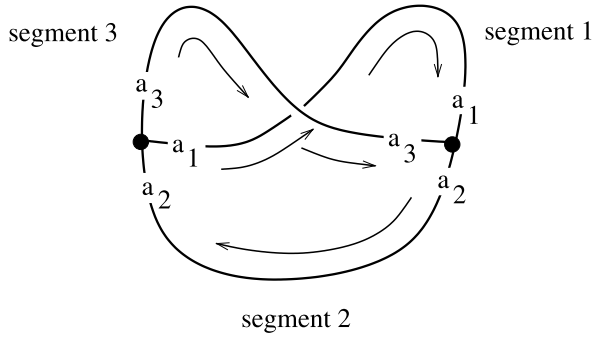

Fig. 26. A graphic which illustrates the rewriting process.

of $B^2 \setminus \{\Delta_i\}$ which contains the matching small singular arc. In this way, the relators are in agreement as well.

EXAMPLE B.1. Equivalence will be demonstrated for a presentation from a previous example. (See Fig. 25.)

ordered presentation: $\{x_1, x_2, y_1, y_2 \mid y_1 = y_2^{-1}x_2y_2,\ x_2 = x_1,\ y_1^{-1}x_1y_1 = y_2\}$,
strings of relators (3, all of length 1): $y_1 = y_2^{-1}x_2y_2 \mid x_2 = x_1 \mid y_1^{-1}x_1y_1 = y_2$,
new generators: a_1, a_2, a_3,
new relators: $a_1 = y_1, a_2 = x_2, a_3 = y_2$,
collapsed presentation: $\{a_1, a_2, a_3 \mid a_1 = a_3^{-1}a_2a_3,\ a_1^{-1}a_2a_1 = a_3\}$.

The collapsed presentation is precisely the LOT presentation for the ribbon disk complement. While working through the previous example, the reader may find Fig. 26 helpful.

ACKNOWLEDGEMENT. The author is grateful to Robert Craggs for many helpful conversations. His description for ribbon disk complements (see Appendix A) is the starting point for the ideas in this article.

References

[1] K. Asano, Y. Marumoto and T. Yanagawa: *Ribbon knots and ribbon disks*, Osaka J. Math. **18** (1981), 161–174.
[2] T. Bedenikovic: *Two-complexes as graph complement cone complexes*, Topology Proc. **27** (2003), 27–38.
[3] C. Cavagnaro: *A homotopy reciprocity law for ribbon disk complements*, Ph.D. thesis, University of Illinois-Urbana, Urbana, IL (1995).
[4] J. Harlander and S. Rosebrock: *Generalized knot complements and some aspherical ribbon disc complements*, J. Knot Theory Ramifications **12** (2003), 947–962.
[5] J. Howie: *On locally indicable groups*, Math. Z. **180** (1982), 445–461.
[6] J. Howie: *Some remarks on a problem of J.H.C. Whitehead*, Topology **22** (1983), 475–485.
[7] J. Howie: *On the asphericity of ribbon disc complements*, Trans. Amer. Math. Soc. **289** (1985), 281–302.
[8] A. Karrass and D. Solitar: *The subgroups of a free product of two groups with an amalgamated subgroup*, Trans. Amer. Math. Soc. **150** (1970), 227–255.
[9] J.G. Ratcliffe: *Free and projective crossed modules*, J. London Math. Soc. (2) **22** (1980), 66–74.
[10] J.H. Remmers: *On the geometry of semigroup presentations*, Adv. in Math. **36** (1980), 283–296.
[11] S. Rosebrock: *On the realization of Wirtinger presentations as knot groups*, J. Knot Theory Ramifications **3** (1994), 211–222.
[12] J.R. Stallings: *A graph-theoretic lemma and group-embeddings*; in Combinatorial Group Theory and Topology (Alta, Utah, 1984), Ann. of Math. Stud. **111**, Princeton Univ. Press, Princeton, NJ., 1987, 145–155.
[13] J.H.C. Whitehead: *On the asphericity of regions in a* 3*-sphere*, Fund. Math. **32** (1939), 149–166.
[14] J.H.C. Whitehead: *On adding relations to homotopy groups*, Ann. of Math. (2) **42** (1941), 409–428.

Department of Mathematics
Bradley University
1501 West Bradley Avenue
Peoria, Illinois 61625
U.S.A.
e-mail: abedenik@bradley.edu